Published in final edited form as:
J Mol Cell Cardiol. 2010 February ; 48(2): 379–386. doi:10.1016/j.yjmcc.2009.09.016.

Excitation-Contraction Coupling Changes during Postnatal Cardiac Development

Andrew P. Ziman[1,2], **Norma Leticia Gómez-Viquez**[1,3], **Robert J. Bloch**[1,2], and **W. J. Lederer**[1,2,4]

[1]Medical Biotechnology Center, University of Maryland Biotechnology Institute, 725 West Lombard St. Baltimore, MD 21201

[2]Department of Physiology, University of Maryland, Baltimore

[3]Departamento de Farmacobiología, CINVESTAV-IPN sede Sur

Abstract

Cardiac contraction is initiated by the release of Ca^{2+} from intracellular stores in response to an action potential, in a process known as “excitation-contraction coupling” (ECC). Here we investigate the maturation of ECC in the rat heart during postnatal development. We provide new information on how proteins of the sarcoplasmic reticulum (SR) and the t-tubules (TTs) assemble to form the structures that support EC coupling during postnatal development. We show that the surface membrane protein, caveolin-3 (Cav3), is a good protein marker for TTs in ventricular myocytes and compared it quantitatively to junctophilin-2 (JP2), a protein found on the SR at sites of SR-TT junctions, or couplons. Although JP2 and Cav3 associate primarily with the SR and TTs, respectively, we found that, they occupy the appropriate sites at maturing structures in synchrony, as visualized with high resolution, quantitative 3-dimensional imaging. We also found the surprising result that while both ryanodine receptor type 2, (RyR2) and JP2 proteins are localized to the same membrane and sub-compartments, they assume their positions at very different rates: RyR2 moves to the SR membrane at the Z-disc very early in development while JP2 only appears in the SR membrane as the TTs mature. Our data suggest that, although RyR2 appears to be prepositioned at the sites ultimately occupied by dyad junctions, JP2 arrives at these sites in synchrony with the development of the TTs at the Z-discs. Finally, we report that EC coupling efficiency changes with development, in concert with these structural changes. Thus we provide the first well-integrated information that links the developing organization of proteins underlying EC coupling (RyR2, DHPR, Cav3 and JP2) to the developing efficacy of EC coupling.

Keywords

excitation contraction coupling; Caveolin 3; Junctophilin 2, calcium induced calcium release; development

Introduction

Cardiac contraction arises as the cardiac electrical signal, or action potential (AP), spreads throughout the heart and triggers an elevation of calcium ($[Ca^{2+}]_i$) which in turn triggers contraction. The components of this excitation-contraction coupling (ECC) process are under tight spatial and temporal control and mature during development [1-6]. Two central elements of the ECC cascade that change with development and disease are the transverse

[4]Corresponding Author.

tubules (TTs) and the sarcoplasmic reticulum (SR) [7-11]. These structures, which underlie ECC, may also de-differentiate in diseased hearts [12, 13].

In mammalian ventricular myocytes, the TT system is incomplete or absent at birth [3, 5, 6, 14]. The appearance of the TT system seems to have both a developmental and evolutionary significance. In ventricular myocytes from birds or fish, the cells are remarkably thin (about 5 microns diameter or less) and have no TTs [15-18]. This makes them similar to atrial myocytes of many adult mammals. The TT system in adult mammalian ventricular myocytes is a specialized system of sarcolemmal invaginations which contain ~80% of the total cellular pool of L-type Ca^{2+} channels (dihydropyridine receptors or DHPRs) [19, 20]. The junctional sarcoplasmic reticulum (jSR), which contains the SR Ca^{2+} release channels of cardiac muscle (ryanodine receptors, RyR2s), is, localized within 15 nm of the regions of the TTs containing DHPRs in adult [21]. The functional units that include DHPRs at the TTs and RyR2s at the jSR form functional units known as couplons [22]. The opening of even one DHPR at a negative membrane potential in a couplon can trigger Ca^{2+} release from a nearby cluster of RyR2s [23, 24]. The activation of a couplon produces a Ca^{2+} spark; the synchronization of many Ca^{2+} sparks by an AP produces the $[Ca^{2+}]_i$ transient that activates contraction [25]. Approximately 80-85% of Ca^{2+} sparks occur within 0.5 microns of the TTs [26, 27].

Here we examine the development of rat ventricular myocytes from postnatal day 10 (d10) to maturity, with the goal of understanding the morphological changes that underlie the development of the apparatus that mediates ECC under normal conditions, and the malfunctions that occur in heart disease. D10 cardiomyocytes lack a TT system and so are structurally immature, compared to adult myocytes, but they develop rapidly, so, by d20 the TT system is indistinguishable from that of adult myocytes. Even at d10, when the TT system is beginning to develop, RyR2s are aligned at the Z-discs. The time-sequence of postnatal development and subcellular organization of ECC proteins is presented here. The precise juxtaposition of key ECC proteins underlies increasing signaling efficiency, as measured by both the peak of triggered $[Ca^{2+}]_i$ and fractional release of SR $[Ca^{2+}]$.

Methods

Developmental Cell Isolation

Cardiac myocytes were isolated from postnatal rats at days 10, 15, or 20 following a protocol modified from Isenberg and Klockner [28]. Briefly, animals were heparinized and anesthetized with pentobarbital prior removal of the hearts by thoracotomy. Once removed, hearts were rapidly bathed in ice cold Ca^{2+}-free Tyrode's solution (containing (in mmol/L) 140 NaCl, 0.5 $MgCl_2$, 0.3 NaH_2PO_4, 5 HEPES, 5.5 glucose, 5 KCl, 0.5 EGTA, pH 7.4) and the aortas were cannulated for Langendorff perfusion. Perfusion to remove blood from the ventricles and circulatory system was at 37°C for 1min with neonatal buffer (NB) solution (containing (in mmol/L) 20 taurine, 70 K-glutamate, 5 pyruvic acid, 40 KCl, 25 HEPES, 1 $MgSO_4$, 10 KH_2PO_4, 22 glucose, pH 7.4) supplemented with 0.1mM EGTA. Next, hearts were digested for 7-12 min with NB + 0.5-1 mg/mL collagenase type 2 (Worthington) and then perfused again with NB + 0.1 mM EGTA for 2 min to remove any residual collagenase. The ventricles were then removed and gently minced in NB + 0.1 mM EGTA. The tissue pieces were triturated to dissociate the myocytes and the cell suspension was filtered through 200 μm nylon mesh. The isolated cells were kept in NB + 1 mM EGTA for 1hr at 4°C to allow them to recover prior to plating.

Adult Cell Isolation

Adult myocytes were isolated from rats at least 8 weeks old, as described [9].

T-tubule Imaging

The sarcolemma and t-tubules (when present) were visualized with the lipophilic fluorescent indicator, Di-8-ANEPPS (Invitrogen Corp. Carlsbad, California). The indicator was initially dissolved to 10 mM in DMSO and applied to freshly isolated myocytes at a final concentration of 10 μM for 5 min at room temperature. Following incubation, the indicator was immediately washed out and the cells were observed by confocal microscopy. Z-stacks were reconstructed into 3-dimensional projections with Volocity version 4.0 (Improvision, Inc.).

Immunofluorescence and Analysis

Freshly isolated myocytes were fixed in 2% paraformaldehyde for 15 min and then washed every 15 min for a total of 4 washes in PBS. Myocytes were incubated in a solution of 1% bovine serum albumin (BSA), 1% normal goat serum (NGS), and 1 mg/mL saponin in phosphate buffered saline (PBS) for 1hr at RT. Cells were incubated with primary antibodies in 1% BSA, 1% NGS, in PBS overnight at 4°C, then washed 4 times every 30 min with 1% BSA, 1% NGS, in PBS, and incubated in secondary antibodies in the same solution for 2 hr at room temperature. After a final series of washes (every 30 min for 3 washes in 1% BSA, 1% NGS in PBS, then 2 times 15 min each in PBS), samples were mounted on glass slides in Slow Fade Lite (Invitrogen Corp.). Negative controls were produced by the same protocol without the use of a primary antibody.

Primary antibodies include monoclonal anti-caveolin 3 (Transduction Labs/BD Biosciences, San Jose, CA), monoclonal anti-ryanodine receptor 2 (Affinity BioReagents, Golden, CO), and polyclonal anti-junctophilin 2 (Zymed, San Francisco, California). Secondary antibodies used here were goat anti-mouse Alexa488 and goat anti-rabbit Alexa633, both from Invitrogen.

Analysis of images for colocalization of pairs of marker proteins was completed using Volocity version 4.0. To compare two proteins in an X-Y image, quantifications of overlap were completed by generating a scatter plot of pixel intensity with one channel (representing one protein) on each axis. After linear regression analysis, a Pearson's correlation (PC) coefficient was calculated to describe the colocalization or variance of the two proteins being tested [29]. More detailed analysis of colocalization was completed by calculating a Manders coefficient for each protein to be localized. This analysis calculates the coefficient of colocalization for each specific marker in the image to quantify the contribution of each marker towards voxels (3-D pixel volumes) containing both markers [30]. Briefly, the software records the fluorescence of each marker in a given volume (voxel by voxel) and compares the colocalized fluorescence to the total fluorescence. These values provide the fraction of colocalized protein divided by total protein in a given volume, or the portion of total fluorescence from a single marker that is found in colocalized voxels.

Ca^{2+} Recording

Freshly isolated myocytes were loaded at room temperature for 30 min with 10μM Fluo-4 AM (stock in 20% pleuronic F127/DMSO). Dye-loaded cells were then perfused with normal Tyrode's solution and voltage clamped in the whole-cell configuration with a HEKA EPC-9 amplifier. The internal bathing solution consisted of (in mmol/L) 130 CsCl, 5 MgATP, 10 HEPES, and 20 TEA. The extracellular solution during patch experiments contained (in mmol/L) 140 NaCl, 0.5 $MgCl_2$, 0.3 NaH_2PO_4, 5 HEPES, 5.5 glucose, 1.8 $CaCl_2$, and 5 CsCl. Once access to the cytoplasm was achieved, the cells were maintained at −80 mV until the protocol called for changes in voltage. SR load was normalized with a voltage protocol including 5 voltage steps from −80 mV to 0 mV at 1 Hz. Voltage-gated Na^+ channels were inactivated by a ramp from −80mV to −50 mv. From −50 mV, 200 ms

voltage steps in 10 mV increments were conducted with simultaneous recording of cell fluorescence.

Imaging

All image acquisition was completed on a Zeiss LSM 510 laser scanning confocal microscope (Zeiss, Inc., Poughkeepsie, NY) with a 63 x water objective and excitation lasers at 488 nm and 633 nm wavelengths. During the acquisition of all two-color images, the multitrack mode was utilized to reduce bleed-through of emitted fluorescence. All X-Y images were captured with a pixel size of no larger than 0.1 μm × 0.1 μm. Z-stack images were recorded with the same X-Y pixel size and a z-step of 0.2 μm.

Statistics

Statistical significance was assessed by ANOVA analysis of all data points with pair-wise comparisons completed as a post-test, with significance defined as a P-value <0.05. Data points represent mean ± SE.

Results

We used postnatal rat ventricular myocytes (d10 – adult) to examine the ontogeny of ECC. Three aspects of the process of development of ECC are relevant to this work: 1. formation of TTs; 2. apposition of TTs and jSR; and 3. maturation of ECC. This work investigates how the alignment of TTs and jSR occurs during development, and underlies the changes in ECC that accompany it.

T-Tubule Formation during Postnatal Development

Although TTs are absent from newborn rat cardiac myocytes [31], they can be readily visualized during development with lipophilic indicators such as di-8-ANEPPS [32]. Using this dye, we obtained high resolution confocal “z-stack” images of myocytes from rat hearts of each age studied (d10 to adult), to create 3-dimensional representations of t-tubule structures. These images show that the TTs appear to sprout inwards from the SL membrane during development. At day 10 (Fig.1 A, B, C), TTs are barely visible as small membranous invaginations near the cell surface. By day 15 (Fig. 1 D, E, F), TTs can be found throughout the cell volume, but they are sparse and do not appear as punctate elements at the Z-disc, as they do in more mature, d20 (Fig.1 G, H, I) and adult (Fig.1 J, K, L) myocytes.

Couplon Assembly in Developing Myocytes

A couplon is the elementary unit of ECC, composed of one or more DHPRs and a cluster of RyR2 (type 2 ryanodine receptors) that assemble at the junction of a TT and a jSR. To establish and quantify their formation in developing cardiomyocytes, we used antibodies to three proteins that represent distinct components of couplons; caveolin 3 (Cav3), a TT marker; RyR2, a jSR marker, and junctophilin-2 (JP2) a marker of the TT-SR junction Cav3, the primary cardiac isoform of caveolin, associates with cholesterol-rich regions of the surface membranes, termed caveolae, and associates with diverse structural, channel and regulatory proteins [33-36]. Cav3 may also play an important role in organizing and maintaining the TT system in cardiac myocytes [37, 38]. JP2 is thought to span the space lying between the TT and the jSR, to connect the two membranes [39, 40]. Colocalization of Cav3 with JP2 (Fig. 2) or RyR with JP2 (Fig. 3) in myocytes of different postnatal ages provided a measure of the changing relationship between the TTs and jSR as myocytes mature.

Cav3 and JP2 Co-localize at TTs. Changes in immunofluorescence labeling for Cav3 illustrate how the surface membrane and TT system mature with development (Fig. 2A, D, G, and J). The developmental changes observed with this marker are similar to those

observed with di-8-ANEPPS (Fig. 1), but the use of Cav3 as a marker allowed us to examine fixed samples. Comparisons of Cav3 labeling with that for JP2 show that these two proteins change similarly during development (Fig. 2). In d10 myocytes, JP2 immunostaining is largely limited to the SL (Fig. 2B), as is Cav3 (Fig. 2A); there is little or no label for either protein within the volume of the cell (Fig. 2B). The merged image of the Cav3 and JP2 immunofluorescence images from d10 cardiomyocytes shows that the two proteins have very similar distributions (Fig. 2C). We provide quantitative comparisons of these distributions below.

As the rat ventricular myocyte matures and Cav3 is found increasingly at intracellular locations at the TTs, at the level of the Z-discs, it also remains at the surface SL (See Figs. 2A, D, G and J). JP2 reorganizes during development in a somewhat different manner. Like Cav3, it accumulates preferentially where TTs are found within the cell, but it is present at diminishing levels at the SL (Fig. 2E, H, K). Overlay images show that, as Cav3 increasingly marks TTs forming within the volume of the cell, JP2 populates the same or nearby regions (Fig. 2F, I, L). In day 20 and adult myocytes, the distributions of Cav3 and JP2 appear to overlap at the level of the TTs, and, although both are found at the SL, there is relatively little JP2 there compared to Cav3 (Fig. 2I, L). This finding is consistent with the current view that couplons are largely found along the TTs in adult myocytes, and less so at peripheral couplings at the SL [20, 21, 24, 26, 27].

RyR2 and JP2 Co-localize in Adult Myocytes. Even at d10, when TTs are largely unformed in rat ventricular myocytes, RyR2s are present in striated patterns at the level of the Z-discs (Fig. 3A). By contrast, JP2 is primarily found at the surface membrane (Fig. 3B). As discussed above, its limited presence within the interior of the cell appears to be restricted to structures adjacent to TTs. Thus, there is little overlap in the distribution of JP2 and RyR2 at d10 (Fig. 3C). With development, however, JP2 concentrates increasingly at the level of the TT and is present in diminishing amounts at the SL. As this occurs, coincidence of labeling for RyR2 and JP2 increases throughout the volume of the cell, particularly in punctate structures adjacent to the Z-discs near the SL (Fig. 3C, F, I, L). These results suggest that, as myocytes develop, JP2 begins to appear adjacent to the Z-discs in close spatial proximity to the RyR2s and this new population of JP2 increases as TTs mature.

Correlation and Colocalization Analysis. We used statistical measures of colocalization to assess the relationships between Cav3 and JP2, and between RyR2 and JP2. Pearson's coefficients (PC) were calculated from myocytes at different postnatal ages that had been co-immunostained for each pair of proteins (Fig. 4A and B). Consistent with the observation that Cav3 and JP2 have very similar patterns of distribution, PCs calculated for Cav3 and JP2 showed no significant differences between them at any of the time points we tested (Fig. 4A). In sharp contrast to this result, PC values calculated for the relationship between RyR2 and JP2 increased during development (Fig. 4B). These results indicate that JP2 and Cav3 become concentrated in intracellular structures as the TT system develops, and that as they do so, their spatial distribution becomes very similar to that of the RyR2.

Whereas the determination of PCs provides a useful statistic of overall correlation of two labeled proteins, analysis using the methods of Manders et al [30] provides more specific assessment of colocalization throughout the volume of the cell or in selected regions (Fig. 4C) by calculating the contribution of each molecule to colocalized volumes. We used this method to analyze the specific voxel content of RyR2 and JP2 visualized in high resolution z-stacks of immunolabeled cells. The contribution of JP2 to colocalization with RyR2 was consistently ~90% (or a coefficient of ~0.9) across all ages and regions (data not shown), but the contribution of RyR2 to colocalization increased throughout development. In d10 myocytes, the contribution of RyR to colocalization was greater near the SL (~33%) than in

the middle (~14%) of the cell. By d15, RyR contribution to colocalization in the cytosol (~35%) was equivalent to colocalization near the SL (~30%). As development continued, the contribution of RyR2 to colocalization with JP2 increased in both subcellular regions until it reached ~79% in the cytosol of adult myocytes (Fig. 4C).

CICR and EC Coupling during Development

The literature suggests that I_{Ca}-triggered SR Ca^{2+} release should increase during postnatal development, as cellular organization matures [14, 41]. We studied ECC in postnatal cardiomyocytes by imaging $[Ca^{2+}]_i$ signals and simultaneously recording I_{Ca} using a whole cell patch clamp method.

I_{Ca} and the triggered $[Ca^{2+}]_i$ transient. We investigated the relationship between L-type I_{Ca} and $[Ca^{2+}]_i$ by loading myocytes with Fluo-4 AM and then patch clamping them in the whole cell configuration. Fig. 5 shows the voltage-gated I_{Ca} and the triggered $[Ca^{2+}]_i$ for a voltage step from −50mV to 0mV. Pooled data from a range of voltage steps (−40mV to +50mV) show that current density (pA/pF) increased significantly from day 10 to day 15 (Fig. 5A, B, and F). Current densities in myocytes at d15 and d20 were not significantly different (Fig. 5B, C, and F). The highest current density was recorded from adult myocytes (Fig. 5F). Although current density increased from day 10 to day 15, there was no difference in the $[Ca^{2+}]_i$ ($\Delta F/F_0$) recorded at either age (Fig. 5E). $[Ca^{2+}]_i$ recorded from either d20 or adult myocytes was significantly greater than $[Ca^{2+}]_i$ from either d10 or d15 myocytes.

Ca^{2+} content in the SR during development. The amount of Ca^{2+} within the SR is expected to change with development between postnatal day 10 and adulthood, as cardiomyocytes get larger and the organization of the SR matures. To evaluate total SR $[Ca^{2+}]$, we measured the peak of caffeine-induced (10 mM) $[Ca^{2+}]_i$ transients (Fig. 6B). Ca^{2+} measurements (given as $\Delta F/F_o$) surprisingly showed that there was no change in SR Ca^{2+} content between postnatal d10 and d20 (Fig. 6A). Caffeine-induced $[Ca^{2+}]_i$ transients recorded in adult myocytes were significantly greater (1.5 fold) than in d20 myocytes, however, suggesting that the ability of the SR to store Ca^{2+} increases after d20. To estimate the maturity of ECC in developing myocytes, we calculated the fractional release of triggered $[Ca^{2+}]_i$ elicited by a voltage step from −50 mV to 0 mV (Fig. 6C). In day 10 and day 15 myocytes only ~33% of total SR $[Ca^{2+}]$ was released by depolarization, while day 20 and adult myocytes released ~60%.

Discussion

ECC in the mature adult heart relies on the amplification of a relatively small current flowing through the DHPRs, which triggers RyRs in the closely apposed SR membrane to open, but neonatal myocytes which continue to develop their ECC organization after birth rely on different mechanisms. During embryonic development and through the time of birth, cardiac myocytes in rodents appear to rely on an influx of Ca^{2+} from not only the DHPR, but also T-type Ca^{2+} channels and the Na-Ca^{2+} exchanger (NCX) [42]. SERCA is expressed at much lower levels early in development than in adults, so removal of elevated $[Ca^{2+}]_i$ produced by Ca^{2+} entry and SR Ca^{2+} release is more dependent on NCX and, presumably, the plasmalemmal Ca^{2+} ATPase [43]. We have studied the subcellular changes in organization and efficiency of ECC in postnatal rat cardiomyocytes as they mature and show that ECC increases with the formation and maturation of a TT system and TT-SR couplons. We show that, although the RyR2s of the SR are organized at the Z-discs and are fully capable of Ca^{2+} release early in development, the efficiency by which they are triggered by DHPRs in the TTs changes dramatically during development. More specifically, we show the surprising result that Cav3 which is found at the TTs colocalizes with the jSR protein JP2 throughout development. However, the dramatic increase in ECC efficiency that is a hallmark of the mature adult ventricular myocyte, does not occur until JP2 and RyR2 colocalize. Our results

provide the first time course of the coordinated structural and functional maturation of couplons during postnatal development in rodent heart.

Our results reveal the relationship between the distribution of proteins involved in excitation-contraction coupling and the functional changes that occur with development during the postnatal period in the rat heart. The transverse tubule system is absent at birth and first appears in an extremely primitive form at approximately postnatal day 10^3. The TT system matures over the first three postnatal weeks, when it attains the architecture seen in the adult heart. Although RyR2 organizes at the Z-discs developmentally early in postnatal rat hearts, proteins of the TT (Cav3 and others) appear intracellularly at later times, consistent with their association with sarcolemmal invaginations visualized with di-8-ANEPPS. Our results show that the efficiency of ECC seen in the adult heart requires complete development and alignment of TT and RyR in the SR, and that intermediate stages of development, in which TT and SR development are incomplete, are accompanied by less efficient coupling of excitatory influx of Ca^{2+}, via L-type Ca^{2+} channels, to the RyR-mediated release of Ca^{2+} from the SR.

Caveolin and T-tubule Formation

Caveolins were first identified as structural proteins of caveolae, cholesterol-rich, flask shaped subdomains of the plasma membrane[44]. Cav3 is also believed to play a role in the formation of TTs in cardiac and skeletal muscle during development, but its absence due to homologous recombination does not prevent the formation of TTs in developing mouse heart [37, 38, 45, 46]. In agreement with others, our results show that Cav3 is present at both the SL and developing and mature TTs in cardiac myocytes [37, 38]. Although its role in TTs is unknown, Cav3 provides a useful tool for tracking the formation and maturation of TTs during cardiac development. Similar to results with Di-8-ANEPPS, antibodies to Cav3 only labeled primitive invaginations in day 10 postnatal cardiac myocytes, In older myocytes, both markers revealed the stages of TT formation and their transverse alignment with respect to the contractile apparatus. These results were consistent with our finding that L-type Ca^{2+} current increased from postnatal day 10 to day 15, when TTs form but are not yet aligned transversely.

Our detection of Cav3 in key locations during development of both the TT system and its enrichment at those locations during maturation of ECC suggest a role in normal cardiac development or function. For example Cav3 may modulate the activity of Na/K ATPase, which would likely affect membrane potential and, indirectly, the size of the Ca^{2+} store in the SR [46]. Recent work by Shibata and colleagues has also suggested that variations in caveolae may enable or blunt Na^+ channel function [47, 48]. Further Cav3 colocalizes with both RyR2 and DHPR, but not NCX, in cardiac myocytes, suggesting that Cav3 is found at dyads [39, 47, 48]. Reduction in caveolae by exposure to increasing concentrations of beta-methyl cyclodextrin, which depletes cells of cholesterol, leads to a dose-dependent decrease in the frequency and size of individual Ca^{2+} release events (Ca^{2+} “sparks”) in both smooth and cardiac myocytes [49].

JP2 and RyR Organization

The junctophilin family of proteins links the plasma membrane (PM) to the endoplasmic/sarcoplasmic reticulum (ER/SR) in many types of cells. JPs have a transmembrane domain that anchors them to the ER/SR. Their cytoplasmic sequences bind to the SL or TT [39, 50]. In skeletal muscle, JP1 and JP2 localize to triad junctions, where they mediate the adhesion of TTs and the terminal cisternae of the SR, but only JP2 is found in heart [51, 52]. JP2 localization changes from a peripheral distribution near the SL in immature cardiac myocytes to a concentration in the triad junctions of the SR, aligned with TTs, in mature

myocytes. Although the timing of this redistribution generally parallels that of TT formation, it is slightly delayed, Our results suggest that, during postnatal cardiac development in the rat, JP2 increasingly co-localizes with the RyR2 clusters as the TTs invaginate and acquire their mature organization, consistent with the idea that the mature organization of JP2 depends on the intersection of the forming TTs and concentrations of RyR2, already established in the SR compartments localized around Z-discs. JP2 and its interactions with proteins of the TT are likely to play a significant role in the health of cardiac muscle. For example, JP2 associates with Cav3, and their interaction is down-regulated in cardiomyopathy. Furthermore, mutations in JP2 occur in some patients suffering from hypertrophic cardiomyopathy[51, 53, 54]. Our findings support an important role for JP2 in the maturation of the structures underlying ECC.

Maturation of EC-Coupling

Our results suggest that the SR in postnatal cardiac myocytes may not fully mature until rats approach 3 weeks of age. Bassani and Bassani (2002) showed that cardiac myocytes from newborn rats relied less on the contribution of SERCA for removal of $[Ca^{2+}]_i$ than adult myocytes (75% vs. 92%) [55]. Our data show that SR $[Ca^{2+}]$ load, as measured by peak response to caffeine, is lower at postnatal days 10 and 15 than in day 20 and adults. Measuring the peak response of Fluo-4 to caffeine application is a less quantitative method for measuring SR $[Ca^{2+}]$ load than methods used by others [56], but it greatly simplifies interpretation of the caffeine response and has been recently used by others as an approximation of SR Ca^{2+} load [57, 58]. Although largely a qualitative measure, the results of this experiment support the idea that postnatal maturation of the SR and its ability to store Ca^{2+} is a slow and ongoing process.

The slow maturation of SR $[Ca^{2+}]$ load parallels that of the triggered $[Ca^{2+}]_i$ transient (Fig. 5), where there is an increase in L-type Ca^{2+} current but no change in the triggered SR $[Ca^{2+}]$ release. The implications of this change in current density are of particular significance for the maturation of ECC, as it represents the functional impact of TT formation without couplon formation. Since there are fewer couplons formed in younger cardiac myocytes compared to adults (Fig. 3, 4), any influx of Ca^{2+} ions that occurs will trigger SR Ca^{2+} release at very few local sites. The fractional release of SR Ca^{2+} expected under these conditions should therefore be reduced. We found that the fractional release of SR Ca in myocytes at 10-15 days after birth, to be ~33%, compared to ~60% in adult cells.

Not only does the absence of couplons early in development have an impact on the fractional release of SR Ca^{2+}, but it also affects rise time or rate of rise for the peak of the $[Ca^{2+}]$ transient. As is apparent in the linescan images shown in Fig. 5, myocytes that lack TT-SR junctions (days 10 and 15) reach the peak of the $[Ca^{2+}]$ transient later than more developed myocytes (day 20 and adult). Moreover, more developed myocytes will have more synchronous DHPR-triggered SR Ca^{2+} release while less developed myocytes will rely heavily on $[Ca^{2+}]$ transient propagation to trigger SR Ca^{2+} release. The slower rise time of the $[Ca^{2+}]$ transient in less mature myocytes is not *prima facia* evidence that the SR cannot be readily triggered by local $[Ca^{2+}]_i$. Indeed, when the triggering mechanism is similar, the rise time of the $[Ca^{2+}]_i$ transient is similar as found for caffeine-induced $[Ca^{2+}]$ transients (data not shown).

Our results in adult myocytes confirms the observations of Delbridge, et al. (1997), who calculated an SR fractional release value of 55.4 ± 9.4% for a single action potential [59]. The combination of lower current density, the inefficient local release due to a lack of couplons, and the small SR Ca load all contribute to the lower SR Ca^{2+} release and the immature state of ECC in early postnatal cardiac development.

Finally, our results suggest that the terminal cisternae of the postnatal rat cardiomyocyte is assembled from at least two distinct membrane components, One forms early, assembles around the Z-discs and contains RyR2; the other forms later, as TTs invaginate, and contains JP2. The factors coordinating the assembly of these two components to form the mature terminal cisternae of the SR, as well as those that link the terminal cisternae to the other compartments of the SR, must still be identified.

Reference List

1. Legato MJ. Cellular mechanisms of normal growth in the mammalian heart. II. A quantitative and qualitative comparison between the right and left ventricular myocytes in the dog from birth to five months of age. Circ Res. Feb; 1979 44(2):263–79. [PubMed: 761308]
2. Legato, MJ. The Developing heart clinical implications of its molecular biology and physiology. Nijhoff; Boston: 1985.
3. Olivetti G, Anversa P, Loud AV. Morphometric study of early postnatal development in the left and right ventricular myocardium of the rat. II. Tissue composition, capillary growth, and sarcoplasmic alterations. Circ Res. Apr; 1980 46(4):503–12. [PubMed: 6444555]
4. Tibbits GF, Xu L, Sedarat F. Ontogeny of excitation-contraction coupling in the mammalian heart. Comp Biochem Physiol A Mol Integr Physiol. Aug; 2002 132(4):691–8. [PubMed: 12095856]
5. Smolich JJ. Ultrastructural and functional features of the developing mammalian heart: a brief overview. Reprod Fertil Dev. 1995; 7(3):451–61. [PubMed: 8606956]
6. Sedarat F, Xu L, Moore ED, Tibbits GF. Colocalization of dihydropyridine and ryanodine receptors in neonate rabbit heart using confocal microscopy. Am J Physiol Heart Circ Physiol. Jul; 2000 279(1):H202–H209. [PubMed: 10899057]
7. Louch WE, Bito V, Heinzel FR, Macianskiene R, Vanhaecke J, Flameng W, et al. Reduced synchrony of Ca2+ release with loss of T-tubules-a comparison to Ca2+ release in human failing cardiomyocytes. Cardiovasc Res. Apr 1; 2004 62(1):63–73. [PubMed: 15023553]
8. Balijepalli RC, Lokuta AJ, Maertz NA, Buck JM, Haworth RA, Valdivia HH, et al. Depletion of T-tubules and specific subcellular changes in sarcolemmal proteins in tachycardia-induced heart failure. Cardiovasc Res. Jul 1; 2003 59(1):67–77. [PubMed: 12829177]
9. Song LS, Sobie EA, McCulle S, Lederer WJ, Balke CW, Cheng H. Orphaned ryanodine receptors in the failing heart. Proc Natl Acad Sci U S A. Mar 14; 2006 103(11):4305–10. [PubMed: 16537526]
10. Currie S, Smith GL. Enhanced phosphorylation of phospholamban and downregulation of sarco/endoplasmic reticulum Ca2+ ATPase type 2 (SERCA 2) in cardiac sarcoplasmic reticulum from rabbits with heart failure. Cardiovasc Res. Jan; 1999 41(1):135–46. [PubMed: 10325961]
11. O'Rourke B, Kass DA, Tomaselli GF, Kaab S, Tunin R, Marban E. Mechanisms of altered excitation-contraction coupling in canine tachycardia-induced heart failure, I: experimental studies. Circ Res. Mar 19; 1999 84(5):562–70. [PubMed: 10082478]
12. Gomez AM, Valdivia HH, Cheng H, Lederer MR, Santana LF, Cannell MB, et al. Defective excitation-contraction coupling in experimental cardiac hypertrophy and heart failure. Science. May 2; 1997 276(5313):800–6. [PubMed: 9115206]
13. Towbin JA, Bowles NE. The failing heart. Nature. Jan 10; 2002 415(6868):227–33. [PubMed: 11805847]
14. Haddock PS, Coetzee WA, Cho E, Porter L, Katoh H, Bers DM, et al. Subcellular [Ca2+]i gradients during excitation-contraction coupling in newborn rabbit ventricular myocytes. Circ Res. Sep 3; 1999 85(5):415–27. [PubMed: 10473671]
15. Myklebust R, Dalen H, Saetersdal TS. A correlative transmission and scanning electron microscopic study of the pigeon myocardial cell. Cell Tissue Res. 1980; 207(1):31–41. [PubMed: 7388911]
16. Bossen EH, Sommer JR, Waugh RA. Comparative stereology of the mouse and finch left ventricle. Tissue Cell. 1978; 10(4):773–84. [PubMed: 746545]
17. Myklebust R, Kryvi H. Ultrastructure of the heart of the sturgeon Acipenser stellatus (Chondrostei). Cell Tissue Res. Nov; 1979 202(3):431–8. [PubMed: 574799]

18. Breisch EA, White F, Jones HM, Laurs RM. Ultrastructural morphometry of the myocardium of Thunnus alalunga. Cell Tissue Res. 1983; 233(2):427–38. [PubMed: 6616575]
19. Brette F, Orchard C. T-tubule function in mammalian cardiac myocytes. Circ Res. Jun 13; 2003 92(11):1182–92. [PubMed: 12805236]
20. Takagishi Y, Yasui K, Severs NJ, Murata Y. Species-specific difference in distribution of voltage-gated L-type Ca(2+) channels of cardiac myocytes. Am J Physiol Cell Physiol. Dec; 2000 279(6):C1963–C1969. [PubMed: 11078712]
21. Franzini-Armstrong C, Protasi F, Ramesh V. Shape, size, and distribution of Ca(2+) release units and couplons in skeletal and cardiac muscles. Biophys J. Sep; 1999 77(3):1528–39. [PubMed: 10465763]
22. Stern MD, Pizarro G, Rios E. Local control model of excitation-contraction coupling in skeletal muscle. J Gen Physiol. Oct; 1997 110(4):415–40. [PubMed: 9379173]
23. Santana LF, Cheng H, Gomez AM, Cannell MB, Lederer WJ. Relation between the sarcolemmal Ca2+ current and Ca2+ sparks and local control theories for cardiac excitation-contraction coupling. Circ Res. Jan; 1996 78(1):166–71. [PubMed: 8603501]
24. Cannell MB, Cheng H, Lederer WJ. The control of calcium release in heart muscle. Science. May 19; 1995 268(5213):1045–9. [PubMed: 7754384]
25. Cannell MB, Cheng H, Lederer WJ. Spatial non-uniformities in [Ca2+]i during excitation-contraction coupling in cardiac myocytes. Biophys J. Nov; 1994 67(5):1942–56. [PubMed: 7858131]
26. Lukyanenko V, Ziman A, Lukyanenko A, Salnikov V, Lederer WJ. Functional Groups of Ryanodine Receptors in Rat Ventricular Cells. J Physiol. Jul 12.2007
27. Shacklock PS, Wier WG, Balke CW. Local Ca2+ transients (Ca2+ sparks) originate at transverse tubules in rat heart cells. J Physiol. Sep 15; 1995 487(Pt 3):601–8. [PubMed: 8544124]
28. Isenberg G, Klockner U. Calcium tolerant ventricular myocytes prepared by preincubation in a “KB medium”. Pflugers Arch. Oct; 1982 395(1):6–18. [PubMed: 7177773]
29. Zou KH, Tuncali K, Silverman SG. Correlation and simple linear regression. Radiology. Jun; 2003 227(3):617–22. [PubMed: 12773666]
30. Manders EMM, Verbeek FJ, Aten JA. Measurement of Colocalization of Objects In Dual-Color Confocal Images. JOURNAL OF MICROSCOPY-OXFORD. Mar 1.1993 169:375–82.
31. Carlsson E, Kjorell U, Thornell LE, Lambertsson A, Strehler E. Differentiation of the myofibrils and the intermediate filament system during postnatal development of the rat heart. Eur J Cell Biol. Apr; 1982 27(1):62–73. [PubMed: 6211355]
32. Kirk MM, Izu LT, Chen-Izu Y, McCulle SL, Wier WG, Balke CW, et al. Role of the transverse-axial tubule system in generating calcium sparks and calcium transients in rat atrial myocytes. J Physiol. Mar 1; 2003 547(Pt 2):441–51. [PubMed: 12562899]
33. Shibata EF, Brown TL, Washburn ZW, Bai J, Revak TJ, Butters CA. Autonomic regulation of voltage-gated cardiac ion channels. J Cardiovasc Electrophysiol. May; 2006 17(Suppl 1):S34–S42. [PubMed: 16686680]
34. Williams TM, Lisanti MP. The caveolin proteins. Genome Biol. 2004; 5(3):214. [PubMed: 15003112]
35. Schlegel A, Lisanti MP. The caveolin triad: caveolae biogenesis, cholesterol trafficking, and signal transduction. Cytokine Growth Factor Rev. Mar; 2001 12(1):41–51. [PubMed: 11312118]
36. Song KS, Scherer PE, Tang Z, Okamoto T, Li S, Chafel M, et al. Expression of caveolin-3 in skeletal, cardiac, and smooth muscle cells. Caveolin-3 is a component of the sarcolemma and co-fractionates with dystrophin and dystrophin-associated glycoproteins. J Biol Chem. Jun 21; 1996 271(25):15160–5. [PubMed: 8663016]
37. Parton RG, Way M, Zorzi N, Stang E. Caveolin-3 associates with developing T-tubules during muscle differentiation. J Cell Biol. Jan 13; 1997 136(1):137–54. [PubMed: 9008709]
38. Carozzi AJ, Ikonen E, Lindsay MR, Parton RG. Role of cholesterol in developing T-tubules: analogous mechanisms for T-tubule and caveolae biogenesis. Traffic. Apr; 2000 1(4):326–41. [PubMed: 11208118]
39. Takeshima H, Komazaki S, Nishi M, Iino M, Kangawa K. Junctophilins: a novel family of junctional membrane complex proteins. Mol Cell. Jul; 2000 6(1):11–22. [PubMed: 10949023]

40. Takeshima H. Ryanodine receptor and junctional membrane structure. Nippon Yakurigaku Zasshi. Apr; 2003 121(4):203–10. [PubMed: 12777839]
41. Seki S, Nagashima M, Yamada Y, Tsutsuura M, Kobayashi T, Namiki A, et al. Fetal and postnatal development of Ca2+ transients and Ca2+ sparks in rat cardiomyocytes. Cardiovasc Res. Jun 1; 2003 58(3):535–48. [PubMed: 12798426]
42. Tohse N, Seki S, Kobayashi T, Tsutsuura M, Nagashima M, Yamada Y. Development of excitation-contraction coupling in cardiomyocytes. Jpn J Physiol. Feb; 2004 54(1):1–6. [PubMed: 15040842]
43. Liu W, Yasui K, Opthof T, Ishiki R, Lee JK, Kamiya K, et al. Developmental changes of Ca(2+) handling in mouse ventricular cells from early embryo to adulthood. Life Sci. Aug 2; 2002 71(11): 1279–92. [PubMed: 12106593]
44. Parton RG, Hanzal-Bayer M, Hancock JF. Biogenesis of caveolae: a structural model for caveolin-induced domain formation. J Cell Sci. Mar 1; 2006 119(Pt 5):787–96. [PubMed: 16495479]
45. Galbiati F, Engelman JA, Volonte D, Zhang XL, Minetti C, Li M, et al. Caveolin-3 null mice show a loss of caveolae, changes in the microdomain distribution of the dystrophin-glycoprotein complex, and t-tubule abnormalities. J Biol Chem. Jun 15; 2001 276(24):21425–33. [PubMed: 11259414]
46. Liu L, Mohammadi K, Aynafshar B, Wang H, Li D, Liu J, et al. Role of caveolae in signal-transducing function of cardiac Na+/K+-ATPase. Am J Physiol Cell Physiol. Jun; 2003 284(6):C1550–C1560. [PubMed: 12606314]
47. Cavalli A, Eghbali M, Minosyan TY, Stefani E, Philipson KD. Localization of sarcolemmal proteins to lipid rafts in the myocardium. Cell Calcium. Sep; 2007 42(3):313–22. [PubMed: 17320949]
48. Balijepalli RC, Foell JD, Hall DD, Hell JW, Kamp TJ. Localization of cardiac L-type Ca(2+) channels to a caveolar macromolecular signaling complex is required for beta(2)-adrenergic regulation. Proc Natl Acad Sci U S A. May 9; 2006 103(19):7500–5. [PubMed: 16648270]
49. Lohn M, Furstenau M, Sagach V, Elger M, Schulze W, Luft FC, et al. Ignition of calcium sparks in arterial and cardiac muscle through caveolae. Circ Res. Nov 24; 2000 87(11):1034–9. [PubMed: 11090549]
50. Hirata Y, Brotto M, Weisleder N, Chu Y, Lin P, Zhao X, et al. Uncoupling store-operated Ca2+ entry and altered Ca2+ release from sarcoplasmic reticulum through silencing of junctophilin genes. Biophys J. Jun 15; 2006 90(12):4418–27. [PubMed: 16565048]
51. Minamisawa S, Oshikawa J, Takeshima H, Hoshijima M, Wang Y, Chien KR, et al. Junctophilin type 2 is associated with caveolin-3 and is down-regulated in the hypertrophic and dilated cardiomyopathies. Biochem Biophys Res Commun. Dec 17; 2004 325(3):852–6. [PubMed: 15541368]
52. Ito K, Komazaki S, Sasamoto K, Yoshida M, Nishi M, Kitamura K, et al. Deficiency of triad junction and contraction in mutant skeletal muscle lacking junctophilin type 1. J Cell Biol. Sep 3; 2001 154(5):1059–67. [PubMed: 11535622]
53. Matsushita Y, Furukawa T, Kasanuki H, Nishibatake M, Kurihara Y, Ikeda A, et al. Mutation of junctophilin type 2 associated with hypertrophic cardiomyopathy. J Hum Genet. 2007; 52(6):543–8. [PubMed: 17476457]
54. Landstrom AP, Weisleder N, Batalden KB, Bos JM, Tester DJ, Ommen SR, et al. Mutations in JPH2-encoded junctophilin-2 associated with hypertrophic cardiomyopathy in humans. J Mol Cell Cardiol. Jun; 2007 42(6):1026–35. [PubMed: 17509612]
55. Bassani RA, Bassani JW. Contribution of Ca(2+) transporters to relaxation in intact ventricular myocytes from developing rats. Am J Physiol Heart Circ Physiol. Jun; 2002 282(6):H2406–H2413. [PubMed: 12003852]
56. Varro A, Negretti N, Hester SB, Eisner DA. An estimate of the calcium content of the sarcoplasmic reticulum in rat ventricular myocytes. Pflugers Arch. Apr; 1993 423(1-2):158–60. [PubMed: 8488088]
57. Waggoner JR, Ginsburg KS, Mitton B, Haghighi K, Robbins J, Bers DM, et al. Phospholamban overexpression in rabbit ventricular myocytes does not alter sarcoplasmic reticulum Ca transport. Am J Physiol Heart Circ Physiol. Mar; 2009 296(3):H698–H703. [PubMed: 19112098]

58. Wang S, Ziman B, Bodi I, Rubio M, Zhou YY, D'Souza K, et al. Dilated cardiomyopathy with increased SR Ca2+ loading preceded by a hypercontractile state and diastolic failure in the alpha(1C)TG mouse. PLoS One. 2009; 4(1):e4133. [PubMed: 19125184]

59. Delbridge LM, Satoh H, Yuan W, Bassani JW, Qi M, Ginsburg KS, et al. Cardiac myocyte volume, Ca2+ fluxes, and sarcoplasmic reticulum loading in pressure-overload hypertrophy. Am J Physiol. May; 1997 272(5 Pt 2):H2425–H2435. [PubMed: 9176314]

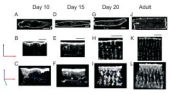

Figure 1. T-tubule Formation and Alignment in Developing Myocytes

The sarcolemma and t-tubules of freshly isolated myocytes were labeled with Di-8-ANEPPS. Single X-Y images of myocytes from postnatal days 10 (A), 15 (C), 20 (E), and adult (G) show an increase in labeling of invaginations of the sarcolemma, identified in subsequent experiments as TTs (white scale bars are 10 μm). 3-Dimensional reconstruction of z-stacks (B, D, F, and H) from the same cells emphasizes the changes in the density of these invaginations and the changes in their organization that occur during development. Black scale bars above each image represent 5 μm.

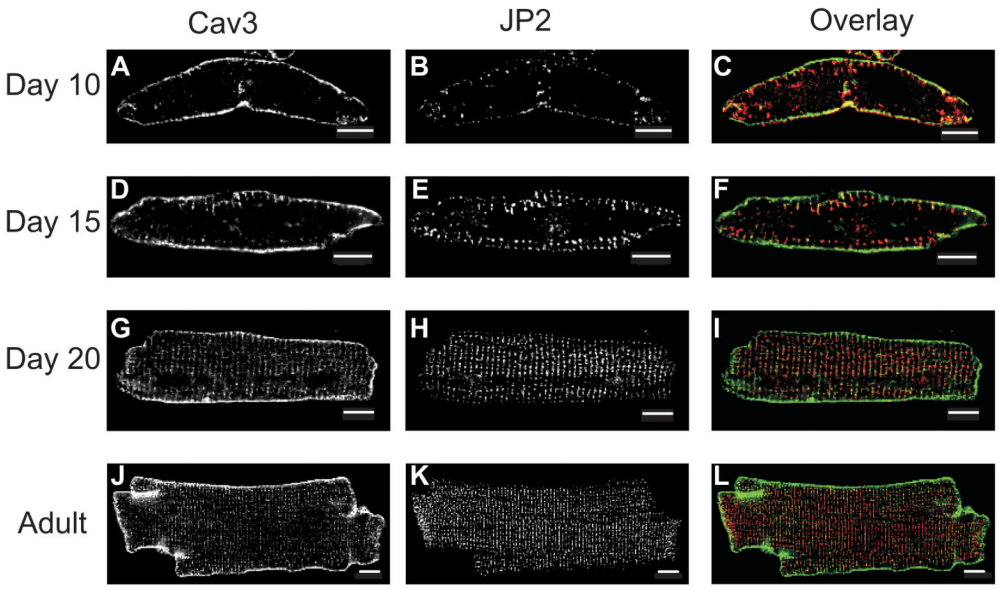

Figure 2. Localization of Caveolin-3 and Junctophilin-2 in Developing Cardiac Myocytes

Ventricular myocytes were fixed and co-immunostained for caveolin-3 (Cav3) and junctophilin-2 (JP2) at postnatal days 10 (A, B), 15 (D, E), and 20 (G, H) and adult (J, K). Overlay images (F, I, L) provide a comparative view of Cav3 (green) and JP2 (red) protein distribution. Scale bars represent 10 μm.

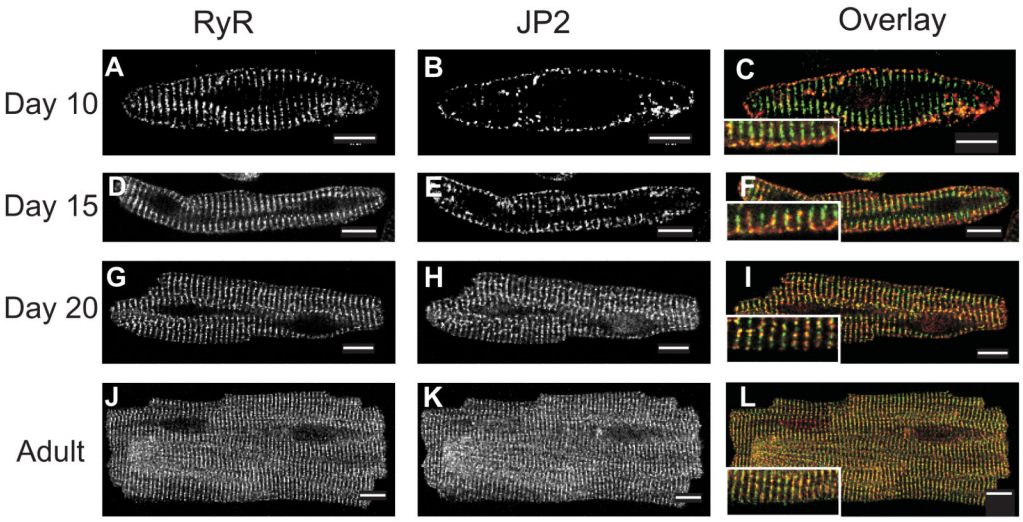

Figure 3. Localization of Ryanodine Receptor-2 and Junctophilin-2 in Developing Cardiac Myocytes

Ventricular myocytes were fixed and co-immunostained for ryanodine receptor-2 (RyR2) and junctophilin-2 (JP2) at postnatal days 10 (A, B), 15 (D, E), and 20 (G, H) and adult (J, K). Overlay images (F, I, L) provide a comparative view of RyR2 (green) and JP2 (red) protein distribution. Scale bars represent 10 μm. Inset images in panels F, I, and L show a zoomed region of the cell.

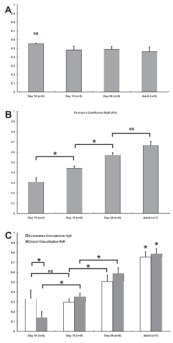

Figure 4. Correlation and Colocalization Analysis of TT-SR Junction Components

A linear correlation analysis was completed to quantify the relationship between Cav3 and JP2 (A) or RyR and JP2 (B). Pearson's coefficients (PCs) calculated for the relationship between Cav3 and JP2 showed no significant difference between any of the time points tested (P-value > 0.05) (A). In contrast, PCs calculated for RyR and JP2 showed a statistically significant (P-value < 0.05) increase at each subsequent time point although there was not significance between day 20 and adult (P-value > 0.05) (B). Further quantification of the spatial relationship between RyR2 and JP2, colocalization analysis was completed by performing a Manders analysis (C). Displayed are the coefficients of colocalization for RyR at regions either near the sarcolemma (open bars) or within the cytosol (closed bars). (Asterisk denotes statistical significance with P-value < 0.05)

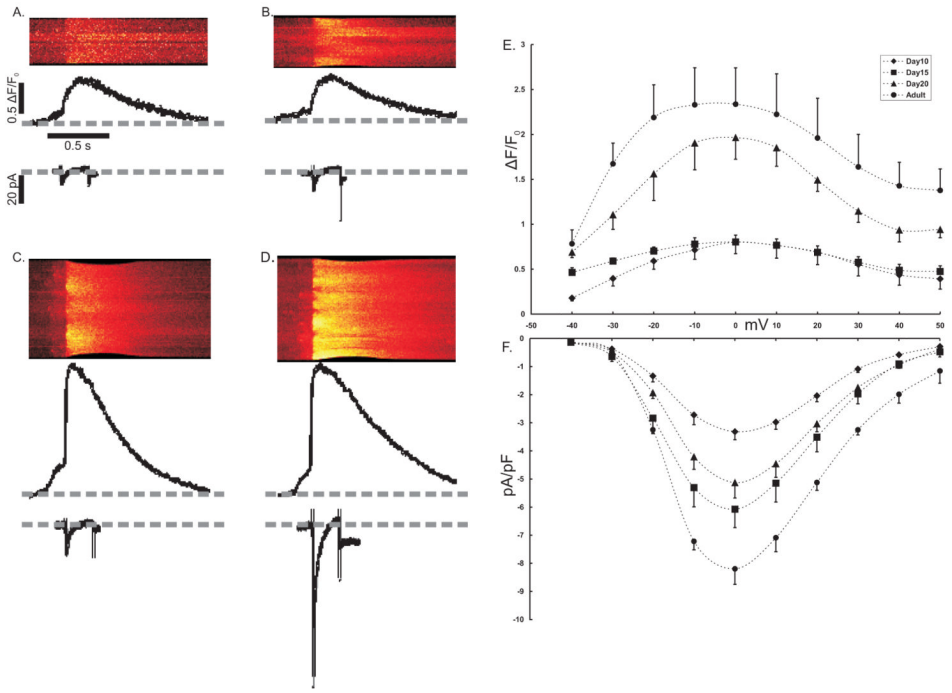

Figure 5. Ca^{2+}-induced Ca^{2+} Release

I_{Ca} and $[Ca^{2+}]_i$ were simultaneously recorded with a whole cell patch clamp method and confocal imaging using freshly isolated myocytes loaded with fluo-4. Whole cell Ca^{2+} transients were recorded during 10mV steps from a holding potential of −50mV. Representative line scan images show $[Ca^{2+}]_i$ recorded during a voltage step to 0mV for each age animal tested (A-D). Beneath the line scan image is a profile of total fluorescence (arbitrary units) from the line scan image and the simultaneously recorded, raw I_{Ca} (pA). Pooled data for the peak of $[Ca^{2+}]_i$ (E) showed no difference between day 10 (◆) (n=6) and day 15 (■) (n=5) myocytes. Although the results obtained from day 20 myocytes (▲) (n=7) were significantly different from these earlier time points, it was not different from values recorded from adult (●) (n=6) myocytes. The corresponding peak I_{Ca} density (I_{Ca} normalized to cell capacitance, pA/pF) showed no difference between days 15 and 20, but both were significantly greater than day 10 and less than adult.

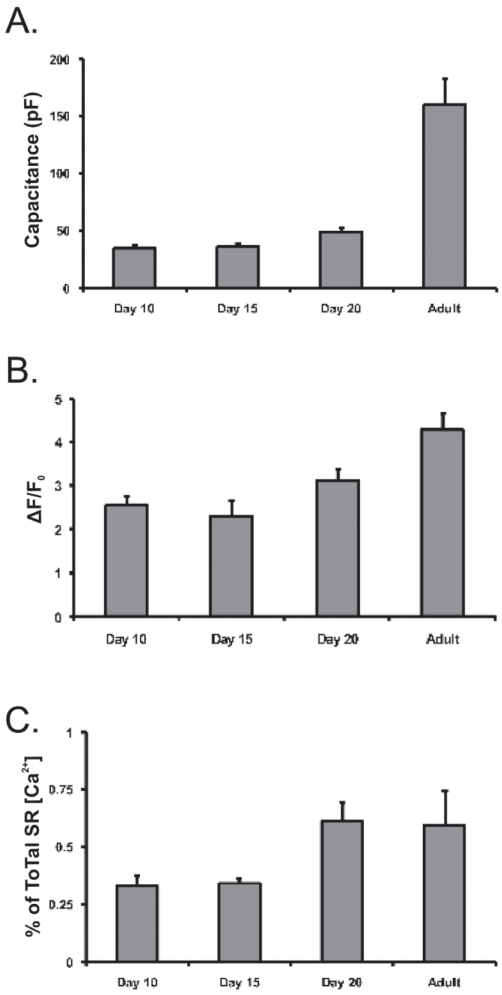

Figure 6. SR Ca^{2+} Content and Triggered Fractional Ca^{2+} Release

Cell size was measured at each developmental time point by recording cell capacitance (pF) (A). Capacitance recordings, calculated by measuring the capacitative current induced by a rapid 10mV hyperpolarizing pulse, shows that cell size was largely unchanged between postnatal day 10 (n=6) and day 15 (n=5). Cells were slightly larger at day 20 (n=7) and considerably larger in adult myocytes (n=6). To measure SR $[Ca^{2+}]$ load (B), freshly isolated ventricular myocytes were loaded with the fluorescent Ca^{2+} indicator, fluo-4. V_m was held constant at −80 mV by whole cell patch clamp while the myocytes were rapidly perfused with a solution of 10 mM caffeine, to induce SR Ca^{2+} release. The recorded peak of the caffeine induced $[Ca^{2+}]_i$ transient ($\Delta F/F_0$) was considered to be a measure of the approximate SR $[Ca^{2+}]$ load. There was no statistical difference between transient peaks recorded in days 10 (n=9) and 15 (n=8) myocytes, while those recorded in day 20 (n=10) were larger ($p<0.001$) and $[Ca^{2+}]_i$ transients recorded in adult (n=5) myocytes were significantly ($P < 0.05$) larger than at all earlier time points. To measure the efficiency of ECC in developing myocytes, fractional SR Ca^{2+} release was calculated by comparing triggered $[Ca^{2+}]_i$ transients to those induced by caffeine application (C). Fractional Ca^{2+} release was smaller in day 10 (n=6) and day 15 (n=8) myocytes at ~33%, than day 20 (n=8) and adult (n=5) myocytes at ~60% ($p<0.05$).